Technical University of Denmark

DTU

# Theory of phase equilibria and critical mixing points in binary lipid bilayers

**Risbo, Jens; Sperotto, Maria Maddalena; Mouritsen, Ole G.**

**DTU Library**
Technical Information Center of Denmark

# Theory of phase equilibria and critical mixing points in binary lipid bilayers

Jens Risbo, Maria M. Sperotto, and Ole G. Mouritsen
*Department of Physical Chemistry, The Technical University of Denmark, Building 206, DK–2800 Lyngby, Denmark*

The fundamental problem of determining the phase equilibria of binary mixtures is discussed in the context of two-component phospholipid bilayer membranes of saturated phospholipids with different acyl-chain lengths. Results are presented from mean-field calculations and Monte Carlo simulations on a statistical mechanical model in which the interaction between lipid acyl chains of different length is formulated in terms of a hydrophobic mismatch. The model permits a series of binary phase diagrams to be determined in terms of a single "universal" interaction parameter. The part of the free energy necessary to derive phase equilibria is determined from the simulations using distribution functions and histogram techniques, and the nature of the phase equilibria is determined by a finite-size scaling analysis which also permits the interfacial tension to be derived. Results are also presented for the enthalpy and the compositional fluctuations. It is shown, in accordance with experiments, that the nonideal mixing of lipid species due to mismatch in the hydrophobic lengths leads to a progressively nonideal mixing behavior as the chain-length difference is increased. Moreover, indications are found that a phase transition in a strict thermodynamic sense may be absent in some of the short-chain one-component lipid bilayers, but a transition can be induced when small amounts of another species are mixed in, leading to a closed phase separation loop with critical points. The physical mechanism of inducing the transition is discussed in terms of the molecular properties of the lipid acyl chains. The results of the numerical model study are expected to have consequences for the interpretation of experimental measurements on lipid bilayer systems in terms of phase diagrams. © *1995 American Institute of Physics.*

## I. INTRODUCTION

Phase equilibria in many-component mixtures are governed by the free-energy function which, however, usually is never readily available from either experiment or theoretical calculation. In particular, under experimental circumstances, usually only first derivatives of the free energy, such as densities and order parameters (e.g., spectroscopic), or second derivatives, such as specific heats and susceptibilities, are experimentally accessible. The phase equilibria then have to be derived indirectly from the behavior of such derivatives, e.g., from changes in the temperature and composition dependence of the densities or order parameters and in particular from possible singular features in the response functions.[1] Generally, the accuracy of the phase equilibria, e.g., in terms of a phase diagram, obtained from such an indirect determination depends on how pronounced the first-order nature of the transition is and how perpendicular to the actual phase boundary the chosen thermodynamic path is. The stronger the density and compositional fluctuations of the mixed system, the more delicate it becomes to determine the phase equilibria from derivatives of the free energy. It is particularly difficult to determine the accurate position of phase boundaries for mixtures close to critical mixing points.

In the present paper we are going to discuss a numerical method based on Monte Carlo simulations by which it is possible to derive very accurately the phase equilibria in many-component mixtures. A prerequisite for the application of the method is a statistical mechanical model in terms of a Hamiltonian which describes the mixture. The approach is general but for the sake of simplicity we shall apply it to a particular class of mixtures, phospholipid bilayers, which are

notoriously known to display phase equilibria that are difficult to assess experimentally as well as theoretically.[2] Lipid bilayers are model systems for biological membranes[1,3] and it is important for the understanding of the functioning of membranes, which are complex many-component mixtures, to be able to describe the phase equilibria in simple few-component lipid mixtures in planar bilayer aggregates. Although our methods and results are presented within the context of lipid systems, the approach is fairly general and should prove useful for other mixtures with intricate phase equilibria and for which statistical mechanical models can be formulated.

Lipid bilayers display a number of thermotropic phase transitions[4] of which the main transition is the one which is most intensively studied since it constitutes the lower boundary for the physiologically interesting fluid phase. At the main transition the bilayer is transformed from a low-temperature solid (gel) phase to a high-temperature fluid (liquid-crystalline) phase.[1] The main transition is usually assumed to be a first-order transition associated with strong precursor effects and fluctuations. The phase equilibria in lipid bilayer systems are conventionally studied experimentally by calorimetric[5,6] or spectroscopic means.[7,8]

The nature of the main transition in one-component phospholipid bilayers is still a controversial issue, although it is usually assumed to be of first order.[2,9] There is, however, no clear-cut experimental proof of this, and the usual assumption of a first-order transition is mainly due to the tradition which developed after the original finding by Chapman *et al.*[10] of a very intense and narrow specific-heat peak with a large heat content for phospholipid bilayers at their

main transition temperature, $T_m$. This finding was later accurately quantified in the classical high-sensitivity differential-scanning calorimetry study by Albon and Sturtevant.[11] Nevertheless, there is no single piece of experimental observation which reveals the kind of discontinuities which are usually associated with first-order behavior. In fact, the most recent and accurate calorimetric study[9] leads to the conclusion that the transition is at best weakly first order and possibly there is no transition at all in a strict thermodynamic sense, i.e., the bilayer transition may be close to a critical point. Whether it is on the side of the critical point corresponding to a (weakly) first-order transition or on the side where there is no phase transition in a strict thermodynamic sense may critically depend on details of the particular system. The current picture of a lipid bilayer at its main transition is hence one of a strongly fluctuating system.[2] The strong fluctuations are signalled on the macroscopic level by dramatic peaks in the response functions,[9] strong variations in the order parameters,[12] and anomalous swelling behavior.[13] Microscopically, the fluctuating state is manifested by formation of lipid clusters and domains leading to a heterogeneous lateral structure which is dynamically maintained.[14] It is interesting to note a well-established fact, experimentally as well as theoretically, that the appearance of the main bilayer transition is strongly dependent on small perturbations, such as imperfections, impurities, sample morphology, trans-bilayer interactions, as well as environmental conditions. One of the aims of the present paper is to demonstrate that, if a phase transition is absent in a one-component lipid bilayer, it may well be induced when a second lipid component is introduced even in a very small amount.

In order to shed some light on the question as to how the nature of the main transition in one-component lipid bilayers controls the phase equilibria in mixtures, it is of interest to study a simple and well-defined theoretical model system for a lipid bilayer in which one can systematically unravel the effects of various system parameters on the phase equilibria. The numerical approach described in the present paper is based on a statistical mechanical model of the molecular interactions between lipid molecules in pure bilayers and mixtures. The approach employs a particular combination of (i) the histogram techniques advanced by Ferrenberg and Swendsen[15] to perform reweighting of thermodynamic distribution functions and (ii) the finite-size scaling analysis applied by Lee and Kosterlitz[16,17] to the logarithm of appropriate distribution functions from which the part of the free energy needed to determine phase equilibria can be derived. Histogram- and finite-size scaling techniques have proved indispensable for problems where there has been doubt as to the nature of the phase transition in one-component systems due to strong fluctuations, e.g., Potts models,[16–18] hard-disc models,[19,20] Abrikosov vortex-lattice models,[21] models with randomness,[22] microemulsion models,[23] and models of liquid crystals.[24–26] Recently the approach was applied to study the nature of the main phase transition in some one-component lipid bilayers[27–29] and critical mixing in a lipid-polypeptide mixture.[30] The present paper shows the full potential of the approach when applied to a binary lipid mixture.
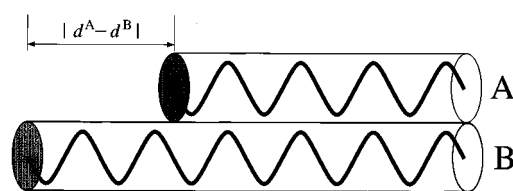


FIG. 1. Schematic illustration of the hydrophobic mismatch between two acyl chains belonging to two different species, A and B, of saturated phospholipid molecules.

The statistical mechanical model on which our numerical study is based is described in Sec. II. Three different mixtures of a homologous series of saturated di-acyl phosphatidylcholines are considered, specifically D14PC-D16PC, D14PC-D18PC, and D12PC-D18PC. (Abbreviations used are D12PC: dilauroyl phosphatidylcholine, D14PC: dimyristoyl phosphatidylcholine, D16PC: dipalmitoyl phosphatidylcholine, D18PC: disteroyl phosphatidylcholine, D20PC: diarachidoyl phosphatidylcholine, corresponding to 12, 14, 16, 18, and 20 carbon atoms in the acyl chain.) Section III describes a mean-field approach to the phase equilibria and a calculation of the system properties at coexistence. The numerical simulation methods are described in Sec. IV, including conventional Monte Carlo simulation in the grand canonical ensemble as well as histogram techniques and finite-size scaling analysis applied to binary mixtures. The results from the numerical simulations are described in Sec. V, and the paper is concluded by a discussion in Sec. VI.

## II. MODEL

The statistical mechanical model used in the present paper for binary lipid mixtures is based on the ten-state Pink model[31] to describe the main transition for each of the pure lipid-bilayer components of the mixture. We consider two different di-acyl lipid species, A and B, which only differ in the length of the acyl chains. The two lipid species are coupled by a term which reflects the incompatibility of acyl chains of different hydrophobic lengths, cf. Fig. 1. This type of hydrophobic mismatch interaction is related to the mismatch interaction of the so-called mattress model of lipid-protein interactions.[30,32,33] The model was also used recently to describe local structure in binary lipid mixtures[34] and binary lipid mixtures incorporated with transmembrane proteins.[35]

The ten-state Pink model for the main transition in one-component lipid bilayers has earlier been described in detail.[31,36,37] Despite its simplicity, the model has proved successful in describing a great variety of physical properties of lipid bilayers and showing how lipids interact with a number of other membrane components.[2] The Pink model describes chain melting on a lattice by taking into account the lipid acyl-chain conformational statistics and the van der Waals interactions between various conformers in a detailed manner, while the excluded volume effect is partially accounted for by assigning each lipid chain to a single site of a trian-

gular lattice. The lipid bilayer is considered as being composed of two noninteracting monolayers. Therefore, the model does not account for possible effects due to chain interdigitation. The acyl chain conformations are represented by ten single chain states, $m = 1,...,10$, each described by a cross-sectional area, $A_m$, an internal energy, $E_m$, and an internal degeneracy, $D_m$. The cross-sectional area is reciprocally related to the hydrocarbon chain length, $d_m$, since the chain volume is approximately invariant under temperature changes. The nine lower states are characteristic of the gel phase and the tenth state is typical of the fluid phase. Of the nine gel states, the lowest state is the all-*trans* ground state and the eight remaining states are low-lying conformational excitations of the ground state. In terms of these variables the Hamiltonian for the ten-state Pink model for lipid species A (and analogously for B) can be written

$$\mathscr{H}^{A} = \sum_i \sum_{m=1}^{10} (E_m^A + \Pi A_m^A) \mathscr{L}_{im}^A$$
$$- \frac{J_A}{2} \sum_{\langle i,j \rangle} \sum_{m,m'=1}^{10} I_m^A I_{m'}^A \mathscr{L}_{im}^A \mathscr{L}_{jm'}^A, \qquad (1)$$

where $\mathscr{L}_{im}^A = 0,1$ is an occupation variable and the pair interactions are extended over nearest-neighbor sites only. The values of the single-chain properties ($E_m^A$, $D_m^A$, $A_m^A$, and $d_m^A$) for di-acyl saturated phosphatidylcholine bilayers have previously been determined by Pink *et al.*[31] $\Pi$ represents an intrinsic effective lateral pressure exerted on a lipid bilayer due to interfacial effects (hydration, polar head interactions, etc.). The interactions between an acyl chain and its six nearest neighbors are given by van der Waals interactions of strength $J_A$ in Eq. (1). $I_m^A$ is a product of a term related to the van der Waals interaction between chains and a phenomenological expression for the shape-dependent nematic parameter.[31] The values of the interaction strengths $J_A$, which we have derived by simple scaling from the previously determined value for D16PC,[36] are as follows: $J_A = 0.5232, 0.618, 0.70985, 0.815, 0.915 \times 10^{-13}$ erg for D12PC, D14PC, D16PC, D18PC, and D20PC, respectively. The parameters $J_{D16PC}$ and $\Pi$ ($=30$ dyn/cm independent of acyl-chain length) were originally found by fitting to experimental values for the transition temperatures and transition enthalpies of pure D16PC.[31,36]

The Hamiltonian function for the binary mixture of the two lipid species A and B is now written

$$\mathscr{H} = \mathscr{H}^A + \mathscr{H}^B + \mathscr{H}^{AB}, \qquad (2)$$

where the two first terms describe the interaction between like species and the last term accounts for the interaction between different species. The interaction between different lipid species is described by the symmetric Hamiltonian

$$\mathscr{H}^{AB} = \frac{-J_{AB}}{2} \sum_{\langle i,j \rangle} \sum_{m,m'=1}^{10} (I_m^A I_{m'}^B \mathscr{L}_{im}^A \mathscr{L}_{jm'}^B + I_m^B I_{m'}^A \mathscr{L}_{im}^B \mathscr{L}_{jm'}^A)$$
$$+ \frac{\Gamma}{2} \sum_{\langle i,j \rangle} \sum_{m,m'=1}^{10} (|d_{im}^A - d_{jm'}^B| \mathscr{L}_{im}^A \mathscr{L}_{jm'}^B$$
$$+ |d_{im}^B - d_{jm'}^A| \mathscr{L}_{im}^B \mathscr{L}_{jm'}^A). \qquad (3)$$

The first term in $\mathscr{H}^{AB}$ describes the direct van der Waals hydrophobic contact interaction between different acyl chains. The corresponding interaction constant is taken to be the geometric average $J_{AB} = (J_A J_B)^{1/2}$. $\Gamma$ in the second term of Eq. (3) represents the mismatch interaction, cf. Fig. 1, and is assumed to be "universal" in the sense that its value does not depend on acyl-chain length. It was previously shown within a two-component regular solution theory[38] that a wide range of binary lipid phase diagrams could be described in terms of such a single universal parameter, once the chain-length characteristics were isolated in the chain-length variables $d_m$. The value of the mismatch parameter to be used within the simulation approach to the statistical mechanics of the model in Eq. (3) was found to be $\Gamma = 0.038 \times 10^{-13}$ erg/Å.[34] In the present paper we shall demonstrate that a similar universal description is furnished by the detailed statistical mechanical model in Eqs. (1)–(3) both within a mean-field solution scheme and when it is solved by a considerably more reliable computer-simulation approach.

Since all of the theoretical results presented in the present work have been derived from the statistical mechanical lattice model described in Eqs. (1)–(3), for which the thermodynamic internal energy and the enthalpy are the same, we shall use these two terms synonymously throughout the paper.

## III. MEAN-FIELD CALCULATIONS

### A. Mean-field theory for binary lipid mixtures

We have modified the mean-field theory previously developed for one-component lipid bilayers and mixtures of lipids with cholesterol[37] to apply to binary mixtures of phospholipids described by the statistical mechanical lattice model in Eqs. (1)–(3). The theory takes its starting point in writing the free energy of the mixture as

$$F = \text{Tr}(\rho \mathscr{H}) + k_B T \text{Tr}(\rho \ln \rho), \qquad (4)$$

where $\rho$ is the equilibrium probability distribution and $\mathscr{H}$ is the Hamiltonian of the model. In the mean-field approximation the $N = L^2$ sites of the two-dimensional lattice are treated as being statistically independent and $\rho$ can therefore be expressed as

$$\rho = \prod_{i=1}^{N} \rho_i, \quad \rho_i = \rho_1, \qquad (5)$$

where $\rho_1$ is the single-site probability distribution. It is then possible to replace $\mathscr{L}_{im}^A$ and $\mathscr{L}_{im}^B$ in the Hamiltonian by their mean values $\langle \mathscr{L}_m^A \rangle$ and $\langle \mathscr{L}_m^B \rangle$. The molar fraction of component B is defined as $x_B \equiv \sum_m \langle \mathscr{L}_m^B \rangle$. The average occupation variables $\langle \mathscr{L}_m^A \rangle$ and $\langle \mathscr{L}_m^B \rangle$ satisfy the completeness relation
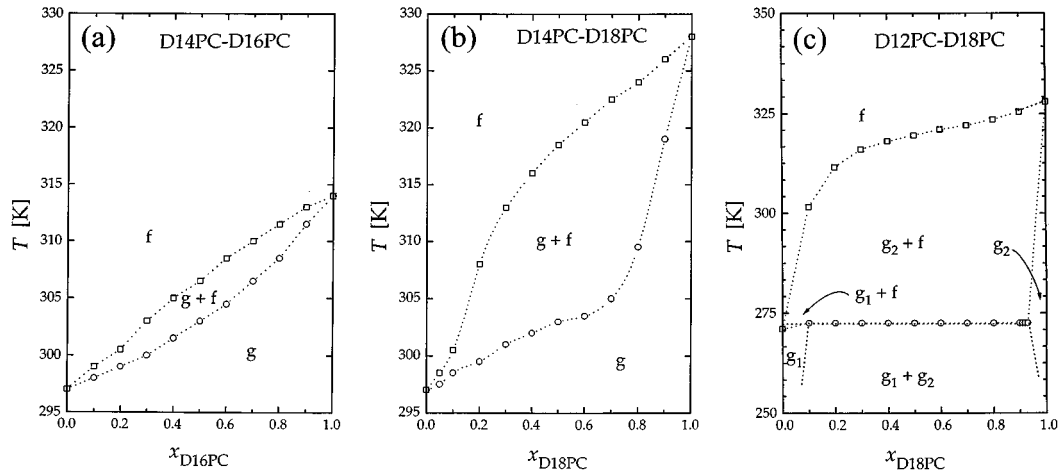
FIG. 2. Phase diagrams for three lipid mixtures determined from mean-field calculations. (a) D14PC-D16PC, (b) D14PC-D18PC, and (c) D12PC-D18PC. The labels denote gel ( **g**, $g_1$, $g_2$) and fluid ( **f**) single-phase regions. Fluid-gel and gel-gel phase coexistence regions are denoted by **g+f**, $g_1$+**f**, $g_2$+**f**, and $g_1$ +$g_2$, respectively.

$\Sigma_m(\langle\mathscr{L}_m^B\rangle+\langle\mathscr{L}_m^A\rangle)=1$. $\rho_1$ is obtained by minimizing the free energy with respect to $\rho_1$ under the constraints $\mathrm{Tr}(\rho_1)=1$ and $\mathrm{Tr}(\Sigma_m\rho_1\mathscr{L}_m^B)=x_B$, i.e.,

$$\frac{\delta}{\delta\rho_1}\left(F+\lambda_1\mathrm{Tr}(\rho_1)+\lambda_2\mathrm{Tr}\left(\sum_{m=1}^{10}\rho_1\mathscr{L}_m^B\right)\right)=0. \quad (6)$$

The Lagrange multipliers $\lambda_1$ and $\lambda_2$ must be chosen so that the constraints are fulfilled. The solution to the minimization problem in Eq. (6) can now be written as

$$\rho_1=\frac{\exp[-(h+\lambda_2\Sigma_m\langle\mathscr{L}_m^B\rangle)/k_BT]}{\mathrm{Tr}(\exp[-(h+\lambda_2\Sigma_m\langle\mathscr{L}_m^B\rangle)/k_BT])}. \quad (7)$$

The mean-field Hamiltonian $h$ in Eq. (7) is defined as

$$h\equiv\frac{1}{N}\frac{\delta}{\delta\rho_1}\mathrm{Tr}(\rho_1\mathscr{H})=\sum_m (h_m^A\mathscr{L}_m^A+h_m^B\mathscr{L}_m^B), \quad (8)$$

where $h_m^A$ and $h_m^B$ are local energies

$$h_m^A=(E_m^A+\Pi A_m^A)-I_m^A\frac{z}{2}\left(J_A\sum_{m'=1}^{10}I_{m'}^A\langle\mathscr{L}_{m'}^A\rangle\right.$$

$$\left.+J_{AB}\sum_{m'=1}^{10}I_{m'}^B\langle\mathscr{L}_{m'}^B\rangle\right)+\Gamma\frac{z}{2}\sum_{m'=1}^{10}|d_m^A-d_{m'}^B|\langle\mathscr{L}_{m'}^B\rangle, \quad (9)$$

(and similarly for $h_m^B$). $z$ is the coordination number ($z=6$ for the triangular lattice). Equation (8) together with the constraint $\mathrm{Tr}(\Sigma_m\rho_1\mathscr{L}_m^B)=x_B$ leads to a determination of the mean value of the occupation variables from a solution to the following set of self-consistent equations

$$\langle\mathscr{L}_m^X\rangle=\mathrm{Tr}(\rho_1\mathscr{L}_m^X)=x_X\left(\frac{D_m^X\exp[-h_m^X/k_BT]}{\Sigma_{m'}D_{m'}^X\exp[-h_{m'}^X/k_BT]}\right),$$

$$X=A,B \quad\text{and}\quad m=1,...,10. \quad (10)$$

The mean-field free energy per lattice site is then expressed as

$$F^{MF}(x_B)=\sum_{m=1}^{10}\left[h_m^A\langle\mathscr{L}_m^A\rangle+h_m^B\langle\mathscr{L}_m^B\rangle+k_BT\right.$$

$$\left.\times\left\{\langle\mathscr{L}_m^A\rangle\ln\left(\frac{\langle\mathscr{L}_m^A\rangle}{D_m^A}\right)+\langle\mathscr{L}_m^B\rangle\ln\left(\frac{\langle\mathscr{L}_m^B\rangle}{D_m^B}\right)\right\}\right]. \quad (11)$$

Finally, the phase diagram in the $(x_B,T)$-plane is obtained by minimizing the function

$$F(x_B,x_1,x_2)=\left(\frac{x_2-x_B}{x_2-x_1}\right)F^{MF}(x_1)+\left(\frac{x_B-x_1}{x_2-x_1}\right)F^{MF}(x_2),$$

$$x_1\leq x_B \quad\text{and}\quad x_2\geq x_B \quad (12)$$

with respect to $x_1$ and $x_2$ for at fixed temperature and composition $x_B$. The values for $x_1$ and $x_2$ determine the phase boundaries of a two-phase coexistence region if they are different from $x_B$.

For each temperature, $T$, the slope of the function $F^{MF}(x_B)$ at $x_B=x_1$, determines the chemical potential difference, $\mu_m^{MF}$, between the two species A, B, corresponding to coexistence. It is hereby possible to derive the phase diagram in the $(\mu_m^{MF},T)$ plane.

## B. Mean-field results for phase diagram, enthalpies, and mixing energies

The mean-field phase diagrams for the three mixtures, D14PC-D16PC, D14PC-D18PC, and D12PC-D18PC, are shown in Fig. 2. The "universal" value of the mismatch parameter used for these mean-field calculations is $\Gamma=0.025\times10^{-13}$ erg/Å which was determined by a fit to the experimental phase diagram for D14PC-D18PC.[6] Figure 2 shows that, as the difference in acyl-chain length is in-
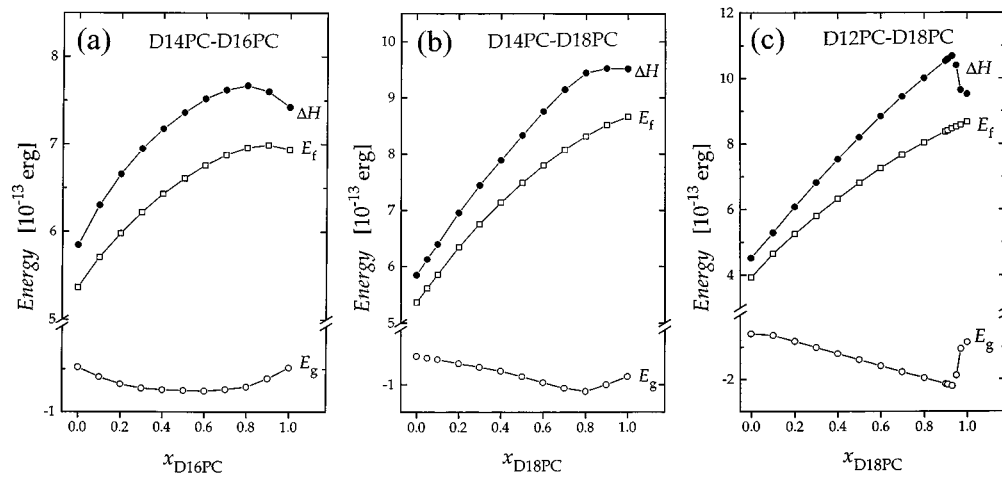
FIG. 3. Mean-field results as a function of composition for the enthalpy along the liquidus, $E_f$ (□), the enthalpy along the solidus, $E_g$ (○), and the transition enthalpy, $\Delta H = E_f - E_g$ (●), cf. the phase diagrams in Fig. 2.

creased, there is a progressive enhancement of the nonideal mixing behavior. The D14PC-D16PC is closest to ideality and there is full mixing in the two phases. For the D14PC-D18PC system this is still the case and the phase behavior is isomorphic but the solidus line is considerably flattened. For an even larger hydrophobic mismatch, the D12PC-D18PC mixture exhibits only limited solubility in the gel phase, and a dramatic peritectic behavior with gel–gel coexistence has evolved. These observations are consistent with previous studies of this homologous series of lipid mixtures.[38,39] In particular we have verified that the phase diagrams for these mixtures can be reproduced reliably by means of a single "universal" parameter $\Gamma$.

The enthalpy (or internal energy) of the two phases at coexistence, $E_g(x)$ and $E_f(x)$, and the transition enthalpy,

$\Delta H(x) = E_f(x) - E_g(x)$, as obtained from the mean-field theory are shown as a function of composition in Fig. 3 for the three mixtures. For the D14PC-D16PC and the D14PC-D18PC mixtures it is found for both components that $E_g$ tends to decrease as small amounts of the other component are mixed in, whereas $E_f$ has a monotonous behavior. This implies that for D14PC-D16PC the transition enthalpy develops a maximum as a function of composition (around 80% D16PC). In the case of D14PC-D18PC the minimum in $E_g$ is only sufficient to produce a flattening of $\Delta H$ close to pure D16PC. The situation for the peritectic mixture, D12PC-D18PC, is somewhat more complicated since small amounts of D12PC in D18PC lead to a dramatic decrease in $E_g$ and subsequent phase separation of the gel phases. This leads to
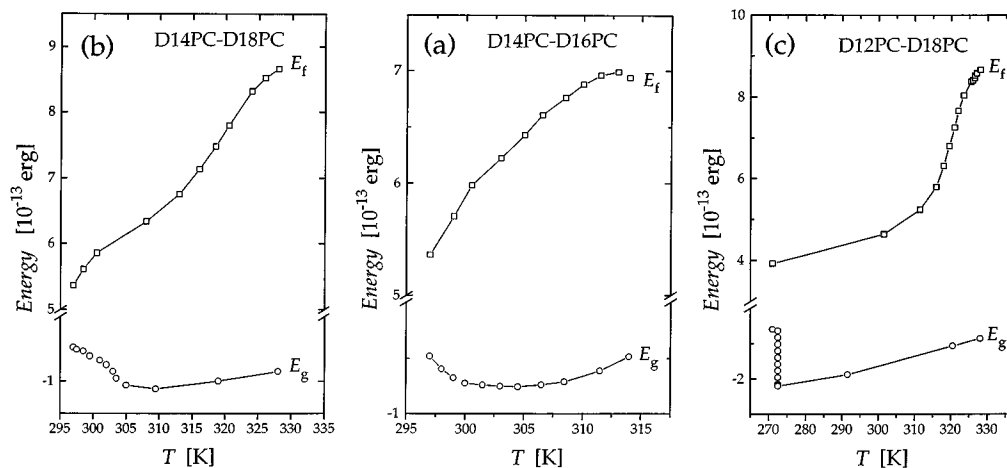


FIG. 4. Mean-field results as a function of temperature for the enthalpy along the liquidus, $E_f$ (□), and the enthalpy along the solidus, $E_g$ (○), cf. the phase diagrams in Fig. 2.

a pronounced maximum in $\Delta H$ around 93% D18PC.

The mean-field enthalpies of the gel and fluid phases, $E_g(T)$ and $E_f(T)$, as functions of temperature along the co-existence curve are shown in Fig. 4. The data for the D12PC-D18PC peritectic mixture again has a special behavior compared to that of the two isomorphic mixtures. The enthalpy of the gel phase, $E_g$, displays a singularity at the three-phase line implying that $E_g$ is not determined by temperature alone but is also dependent on composition. The very dramatic variation in $E_g(x)$ observed over the range 93%–100% of D18PC in Fig. 3(c) is by help of Fig. 4(c) seen to occur over a very wide temperature range of about 60 degrees. A comparison between the phase diagrams for the three mixtures in Fig. 2 as well as the enthalpy data in Fig. 4 shows that as the mismatch in chain length is increased, the phase-separation region gets more pronounced and the two lipid species melt at temperature regions which are increasingly wider apart. This is particularly pronounced for the D12PC-D18PC mixture, cf. Fig. 4(c), where basically all of the short-chain lipid melts within a narrow temperature interval around 273 K and the long-chain lipid predominantly melts in the temperature range 315–330 K.

Previous theoretical model calculations of lipid binary phase equilibria are mostly built on the use of various phenomenological theories of solution, e.g., regular solution theory[39] which is basically a mean-field approach. With these theories it is fairly easy to reproduce experimental phase diagrams with just one or two nonideal interaction parameters for each mixture. However, to accurately reproduce a whole family of different phase diagrams for a series of mixtures using a single common parameter, as was done in Fig. 2, is highly nontrivial.[38] This is one advantage of the present approach. Another advantage is that the present mean-field calculation is performed on a statistical mechanical model which explicitly contains information about the internal degrees of freedom of the acyl chains, whereas this type of information in conventional regular solution theories is hidden in the standard chemical potentials of the different phases. These standard chemical potentials are usually treated as an experimental input to the regular solution theory by using experimental data for transition enthalpies and temperatures and by assuming that the specific heat within the one-phase regions is independent of temperature. In other words, the phenomenological regular solution theories do not provide a description of the transitional properties of the pure components.

The present approach permits a discussion of the phase equilibria in terms of nonideality and how this is controlled by the molecular properties of the involved species. Let us study the results presented in Fig. 3 in the light of deviations from regular solution theory and consider the gel and fluid components of the phase coexistence as being mixtures of the gel and fluid phases of the pure components. Under this assumption the enthalpy of the mixture can be written

$$E(x,T) = xE^{\circ}_{B,\alpha} + (1-x)E^{\circ}_{A,\alpha} + E_{mix}(x,T), \qquad (13)$$

where the enthalpies of the pure phases are denoted by $E^{\circ}_{X,\alpha}$, which are assumed to be constant and evaluated at the

appropriate transition temperature, X=A,B and $\alpha$=g,f. $E_{mix}$ is a nonideal mixing enthalpy which not only includes nonideal interaction energies but also the variation of the lipid-chain conformational energy due to temperature changes and mixing. In a similar fashion the entropic contribution to the free energy is written

$$-TS(x,T) = -T[xS^{\circ}_{B,\alpha} + (1-x)S^{\circ}_{A,\alpha} + S_{mix}(x,T)], \qquad (14)$$

where $S^{\circ}_{X,\alpha}$ is the entropy of the pure component X in phase $\alpha$ and is assumed to be temperature-independent and determined at the appropriate transition temperature. Within the mean-field picture the compositional part of the mixing entropy is just that of an ideal mixture. Hence the total mixing entropy, $S_{mix}(x,T)$, in Eq. (14) can be written as a sum of the ideal mixing entropy and a contribution, $S_{chain}$, which is due to the internal conformational degrees of freedom of the acyl chains

$$S_{mix}(x,T) = S_{ideal}(x) + S_{chain}(x,T). \qquad (15)$$

Within this description $S_{chain}$ is the deviation from the mixing entropy of an ideal mixture. In Fig. 5 are given the various entropy terms together with the mixing enthalpy for three typical cases. Figures 5(a) and 5(b) give results along the solidus line for the D14PC-D16PC and D14PC-D18PC mixtures. The corresponding results for the solidus line for the D12PC-D18PC mixture are not shown since this mixture does not mix in the gel phase except at low compositions. Figure 5(c) shows instead the results along the liquidus line of the D14PC-D18PC mixture. The results for the liquidus of the two other mixtures are qualitatively very similar and are hence not shown.

An important observation to be made from the data in Fig. 5 is that the real mixture displays a significantly enhanced transition enthalpy compared to that of an ideal mixture. Furthermore, it is found that the deviation from ideality is stronger for small amounts of D14PC in D18PC than for small amounts of D18PC in D14PC. This is apparently in contradiction to the conclusion made in a theoretical study by von Dreele[40] based on the Prigogine approximation for the partition function. However, it is difficult to compare the two different theoretical analyses since only the present study takes the internal acyl-chain degrees of freedom into account.

The data displayed in Fig. 5 may serve to facilitate a comparison with results obtained from solution theories in which the temperature variation of the properties of the pure components are neglected. The essential feature of the mixture of lipids seen as molecular species with internal degrees of freedom is that at the entry to the gel phase the acyl chains become conformationally ordered by stretching into a molecular state with a lower internal energy and a lower conformational entropy. This leads to a non-negligible decrease in the total entropy of the mixture. Conversely, at the entry to the fluid phase the acyl chains become conformationally disordered associated with an increase in conformational en-
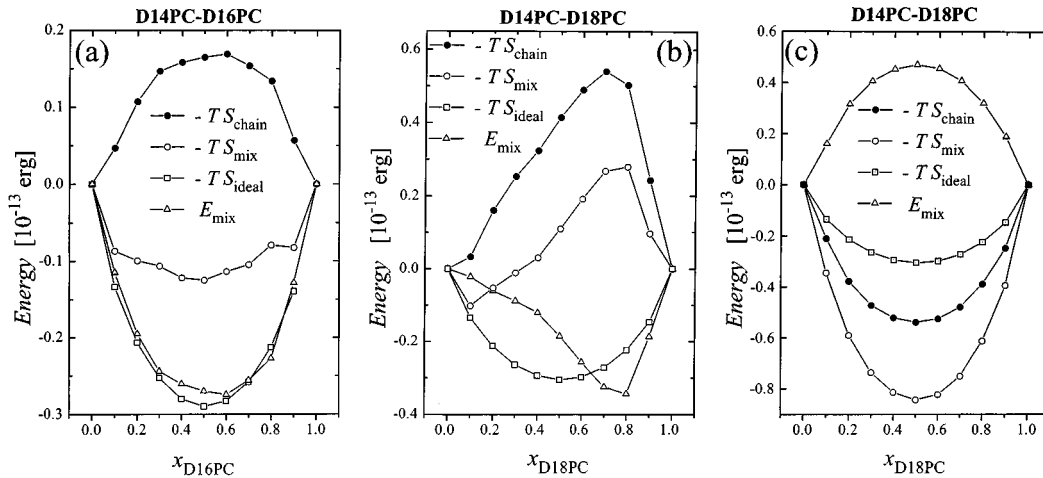
FIG. 5. Mean-field results for the different contributions to the free energy of a binary lipid mixture. Results are shown for the total mixing entropy, $S_{mix}$, the ideal mixing entropy, $S_{ideal}$, and the conformational acyl-chain entropy, $S_{chain}$, cf. Eq. (15). $E_{mix}$ is the nonideal mixing enthalpy, cf. Eq. (13). (a): Along the solidus of the D14PC-D16PC mixture. (b): Along the solidus of the D14PC-D18PC mixture. (c): Along the liquidus of the D14PC-D18PC mixture.

tropy, i.e., a negative contribution to the free energy, whereas the nonideal mixing enthalpy, $E_{mix}$, increases the free energy of the mixture. The consequence of this mixing behavior is that the melting process of the mixed lipid system, compared to that of the pure components, proceeds from a more conformationally ordered state to a more conformationally disordered state. The observed enhancement of the nonideal melting entropy over that of an ideal mixture is hence likely to be due to the mixing behavior of the conformational energy rather than the nonideal interaction energies. In the fluid phase there is some degree of cancellation of the enthalpic and entropic contributions to the free energy implying that the mixture in the fluid phase is closer to an ideal mixture. This suggests that regular solution theory is inappropriate for describing mixtures of lipids due to the substantial contribution of the chain conformational degrees of freedom to the total entropy and the total enthalpy of the mixture.

## IV. NUMERICAL SIMULATION METHODS

### A. Monte Carlo techniques

The Monte Carlo simulations are carried out on finite lattices subject to periodic boundary conditions. In order to determine system properties in the thermodynamic limit, a series of different linear lattice sizes, $L$, have been investigated. The simulations are performed within the grand canonical ensemble where the composition of the mixture fluctuates and is controlled by a field, $\mu$, which is the chemical potential difference between the two species. For these simulations Eq. (2) is modified accordingly

$$\mathcal{H} - \mu N_B = \mathcal{H}^A + \mathcal{H}^B + \mathcal{H}^{AB}, \tag{16}$$

where $N_B$ is the number of lattice sites occupied by component B. The grand canonical simulations provide the distribution functions, see Sec. IV B below, which are used to

assess the phase equilibria and serve as input for the finite-size scaling analysis needed for calculating the interfacial tension, cf. Sec. IV C below. The statistics required to accurately determine the phase coexistence at a given temperature typically involve $10^6$ Monte Carlo steps per lattice site.

The simulations are carried out using standard Monte Carlo Metropolis sampling. Thermal equilibrium of the model system is attained using single-site Glauber excitation for the acyl-chain degrees of freedom on each lipid species. Equilibrium with the particle reservoir within the grand canonical ensemble is simulated by single-site conversion of the lipid species and simultaneous assignment of a random acyl-chain conformation.

### B. Histogram techniques

In order to use the Lee-Kosterlitz finite-size scaling method effectively to study phase equilibria in mixtures, it is a prerequisite that the joint distribution function (or histogram), $\mathscr{P}(E, N_B)$, for the extensive variables, namely internal energy (the enthalpy) and the composition, $N_B$, is calculated very accurately close to coexistence, cf. Sec. IV C. $\mathscr{P}(E, N_B)$ for a given set of thermodynamic parameters $(T, \mu)$ is defined by

$$\mathscr{P}_{T,\mu}(E, N_B) = \frac{n(E, N_B) \exp[-(E + \mu N_B)/k_B T]}{\Sigma_{E,N_B} n(E, N_B) \exp[-(E + \mu N_B)/k_B T]}, \tag{17}$$

where $n(E, N_B)$ is the temperature-independent density of states. If $\mathscr{P}$ is calculated with sufficient accuracy for a specific set, $(T, \mu)$, it is possible[15] to determine the distribution function for a nearby set of parameters, $(T', \mu')$, by simple thermodynamic reweighting of the histogram according to

$$\mathscr{P}_{T',\mu'}(E,N_\mathrm{B}) = \frac{\mathscr{P}_{T,\mu}(E,N_\mathrm{B}) \, \exp\left[-\left(\dfrac{1}{k_\mathrm{B}T'} - \dfrac{1}{k_\mathrm{B}T}\right)E - \left(\dfrac{\mu'}{k_\mathrm{B}T'} - \dfrac{\mu}{k_\mathrm{B}T}\right)N_\mathrm{B}\right]}{\displaystyle\sum_{E,N_\mathrm{B}} \mathscr{P}_{T,\mu}(E,N_\mathrm{B}) \, \exp\left[-\left(\dfrac{1}{k_\mathrm{B}T'} - \dfrac{1}{k_\mathrm{B}T}\right)E - \left(\dfrac{\mu'}{k_\mathrm{B}T'} - \dfrac{\mu}{k_\mathrm{B}T}\right)N_\mathrm{B}\right]}. \tag{18}$$

From the joint, two-dimensional distribution function, $\mathscr{P}(E,N_\mathrm{B})$, the two one-dimensional distribution functions can readily be derived as

$$\mathscr{P}(E) = \sum_{N_\mathrm{B}} \mathscr{P}(E,N_\mathrm{B}), \tag{19}$$

$$\mathscr{P}(N_\mathrm{B}) = \sum_{E} \mathscr{P}(E,N_\mathrm{B}). \tag{20}$$

In Eqs. (17)–(20), $E$ denotes the total internal energy. In the following we shall use the same symbol for the internal energy per molecule.

## C. Finite-size scaling theory

Phase equilibria can be examined by the powerful method of Lee and Kosterlitz.[16,17] This method, which is built on finite-size scaling analyses of distribution functions (histograms) derived from computer simulations, constitutes an unambiguous technique for numerically detecting first-order transitions and phase coexistence.[26] The method involves calculation of a certain part of the free energy using the distribution functions in Eqs. (19) and (20). From these distribution functions, free-energy-like functions, e.g., $\mathscr{F}(x,T,L)$, can be defined as[16]

$$\mathscr{F}(x,T,L) \sim -\ln \mathscr{P}_{T,\mu}(L), \tag{21}$$

where the dependence of the linear system size, $L$, has explicitly been expressed. The quantity $\mathscr{F}$ differs from the total free energy by a temperature- and an $L$-dependent additive quantity. However, at fixed $T$ and $L$, the shape of $\mathscr{F}(x,T,L)$ is identical to that of the total free energy and furthermore $\Delta\mathscr{F}(\mu,T,L) = \mathscr{F}(x,T,L) - \mathscr{F}(x',T,L)$ is a correct measure of free-energy differences. At a first-order transition, $\mathscr{F}(x,T,L)$ has pronounced double minima corresponding to two coexisting phases at $x=x_1$ and $x=x_2$ separated by a barrier, $\Delta\mathscr{F}(\mu,T,L)$, with a maximum at $x_{\max}$ corresponding to an interface between the two phases. The height of the barrier measures the interfacial free energy between the two coexisting phases and is given by

$$\Delta\mathscr{F}(\mu,T,L) = \mathscr{F}(x_{\max},T,L) - \mathscr{F}(x_1,T,L)$$
$$= \gamma(\mu,T)L^{d-1} + \mathscr{O}(L^{d-2}), \tag{22}$$

where $d$ is the spatial dimension of the system ($d=2$ in the present case). $\gamma(\mu,T)$ is the interfacial free-energy density or interfacial tension. Therefore $\Delta\mathscr{F}(\mu,T,L)$ increases monotonically with $L$ at a first-order transition corresponding to a finite interfacial tension. The detection of such an increase is an unambiguous sign of a first-order transition[17]

and two-phase coexistence.[26,30] In contrast, $\Delta\mathscr{F}(\mu,T,L)$ approaches a constant at a critical point, corresponding to vanishing interfacial tension in the thermodynamic limit. In the absence of a transition,[16,27] $\Delta\mathscr{F}(\mu,T,L)$ tends to zero.

## D. Tuning-in at coexistence

The iterative procedure for tuning in at coexistence is as follows: A trial value of the chemical potential at coexistence, $\mu=\mu_m$, for a given temperature is guessed or estimated from a short simulation on a very small lattice. The accurate value of $\mu_m$ for that system size is then determined by a long simulation (typically $10^6$ Monte Carlo steps per lattice site) at this trial value of $\mu$ and a more accurate value of $\mu=\mu_m$ is then determined by the Ferrenberg-Swendsen reweighting technique, cf. Eq. (18). If the trial value turns out to be too far from coexistence to allow a sufficiently accurate sampling of the two phases, a new trial value is estimated from the long simulation. The system size is then increased and the value of $\mu=\mu_m$ for the previous system size is used as trial value for the long simulation on the larger system. After the reweighting, the accuracy of the reweighting procedure is checked by a direct calculation at a chosen value of the chemical potential. This rather tedious and lengthy iterative procedure assures a very accurate determination of the chemical potential at coexistence and hence leads to an accurate determination of the compositional phase diagram via the finite-size scaling analysis described in Sec. IV C.

The Ferrenberg-Swendsen reweighting technique becomes more and more troublesome the larger the size of the system studied because the distribution functions get narrower for larger systems. The method works best for small systems which are subject to large fluctuations allowing more information about a larger part of phase space to be sampled. Reweighting of data obtained for one value of the chemical potential to another value gives a greater uncertainty for the larger system simply because it is the extensive composition that enters the Hamiltonian and hence the reweighting procedure, cf. Eq. (18). This implies that one needs to know the chemical potential at coexistence with an accuracy which varies approximately as $L^{-2}$. Another bottleneck of a more principal and physical nature is the time, $\tau$, associated with the crossing of the free-energy barrier between the two phases. This time increases exponentially with the linear dimension of the two-dimensional model system, $\tau \sim \exp(\gamma L/k_\mathrm{B}T)$. In order to facilitate the reweighting, the actual simulation time has to be much larger than $\tau$. For a given model, the value of this relaxation time puts a very sharp upper limit to the system sizes which can be studied by these simulation techniques.
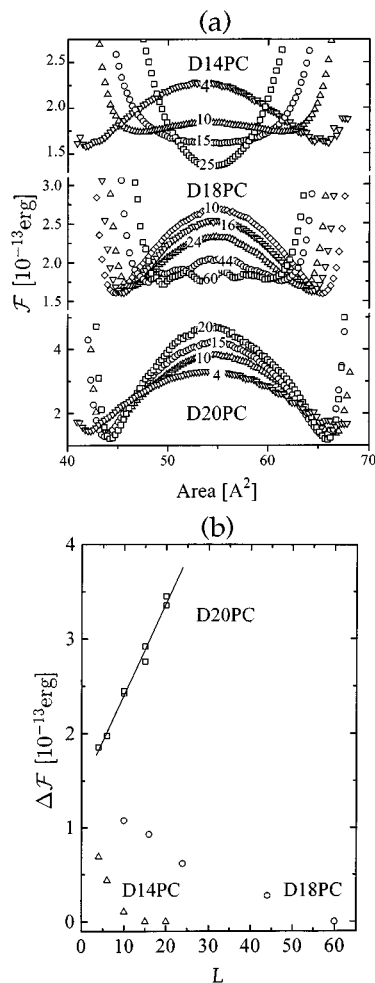
FIG. 6. Monte Carlo results for pure D14PC, D18PC, and D20PC lipid bilayers. (a) Free-energy functional, $\mathscr{F}(A)$, as a function of average cross-sectional area, $A$, per lipid molecule for different system sizes, $L$, as indicated on the curves. (b) Free energy barrier height, $\Delta\mathscr{F}$, as a function of $L$; D14PC ($\triangle$), D18PC ($\bigcirc$), D20PC ($\square$).

## V. SIMULATION RESULTS

Monte Carlo simulations involving histogram techniques and detailed finite-size scaling analysis for determining phase equilibria are very demanding with respect to the statistics. Hence we have not performed detailed simulations for all three mixtures considered by the mean-field calculations above. Instead we have concentrated on a single mixture, D14PC-D18PC, which however clearly illustrates the points we want to make.

From previous simulations using both histogram and finite-size scaling techniques,[29] it is known that the pure lipid bilayers of D16PC, and D18PC described by the ten-state Pink model in Eq. (1) do not display a phase transition in a strict thermodynamic sense but undergo a continuous, nonsingular transformation within a very narrow temperature range. The results for D18PC have been confirmed by the present calculations. For completeness, the phase behavior of D14PC and D20PC has also been investigated. Figure 6(a)

shows the system-size dependence of the free energy $\mathscr{F}$ as a function of the average area per lipid molecule, $A$, for pure D14PC, D18PC, and D20PC lipid bilayers. Figure 6(b) shows the height of the free energy barrier, $\Delta\mathscr{F}(A)$, as a function of $L$. It is found that, as the chain length is increased, the bilayer gets closer to a critical point which is present inbetween chain lengths corresponding to 18 and 20 carbon atoms. For the lipid species with the longest chain length studied, D20PC, we indeed find that there is a clear first-order transition within the ten-state Pink model, as determined by the linear dependence of $\Delta\mathscr{F}(A)$ on $L$.

## A. Histograms, free-energy functionals, and phase equilibria

The bottom graph in Fig. 7(a) shows an example of the compositional distribution function or histogram, $\mathscr{P}(x)$, at a temperature $T = 319$ K for a D14PC-D18PC system of linear size $L = 10$. Results are given before and after reweighting to a chemical potential corresponding to coexistence. The corresponding free energy functional, $\mathscr{F}(x)$, is shown in the top of Fig. 7(a). The size dependence of $\mathscr{F}(x)$ is shown in Fig. 7(b) while Fig. 7(c) shows the size dependence of $\mathscr{F}(E)$, where $E$ is the internal energy (enthalpy) per molecule. The distribution functions are shown at the appropriate size-dependent chemical-potential values corresponding to phase coexistence. As the system size is increased, it is seen that there is a dramatic increase in the free-energy barrier between the two phases and that the composition of the mixture is $x_{\text{D18PC}}^{\text{g}} = 0.95$ and $x_{\text{D18PC}}^{\text{f}} = 0.42$. Similarly, the enthalpy distribution function shows that at coexistence the two phases have enthalpies around $E_{\text{g}} \simeq -1 \times 10^{-13}$ erg/molecule and $E_{\text{f}} \simeq 8 \times 10^{-13}$ erg/molecule.

From the size dependence of the free-energy barrier, $\Delta\mathscr{F}(L)$, shown in Fig. 8 the interfacial tension, $\gamma$, can be calculated using Eq. (22). From the plot in Fig. 8, $\gamma$ is determined to be $\gamma = 0.57 \times 10^{-13}$ erg/lattice unit.

The simulation data shown in Fig. 7 correspond to a temperature $T = 319$ K where the D14PC-D18PC mixture exhibits a clear first-order transitional behavior associated with two-phase coexistence. Figures 9(a) and 9(b) show data for the free energy-functional, $\mathscr{F}(x,L)$, and the free-energy barrier, $\Delta\mathscr{F}(L)$, for lower temperatures. This data set demonstrates that the model for the D14PC-D18PC mixture exhibits a critical mixing point at a certain temperature. Figure 9(b) shows unequivocally, that the free-energy barrier decreases with system size at $T = 299.0$ K and lower temperatures indicating that the interfacial tension vanishes and there is no phase transition or phase coexistence in the thermodynamic limit. Conversely, the data for $T = 299.5$ K and higher temperatures shows a free-energy barrier that increases with system size and hence phase coexistence prevails in the thermodynamic limit. Hence, the combined data set in Fig. 9(b) strongly suggests that there is a lower critical mixing point at a temperature between $T = 299.0$ and $299.5$ K. By a similar type of analysis we have found that there is an upper critical mixing point at a temperature, $T \simeq 327$ K.
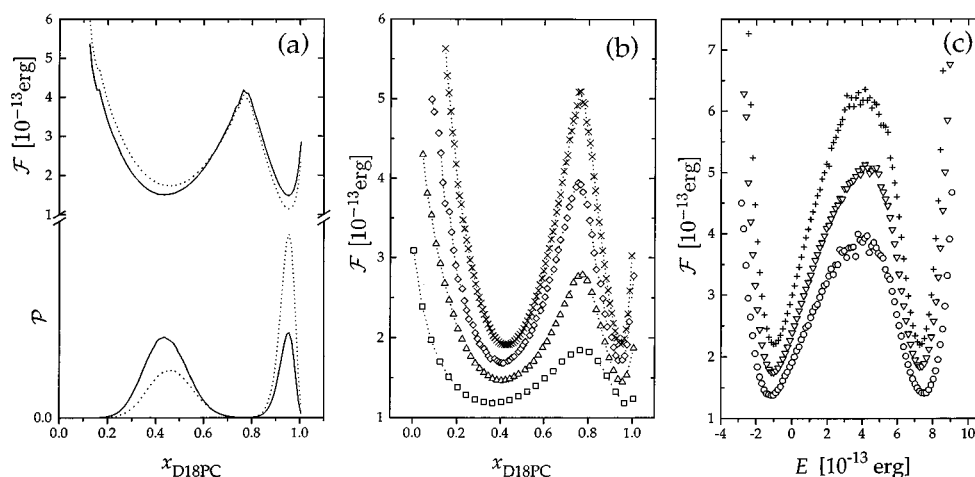
FIG. 7. Monte Carlo computer-simulation data for the D14PC-D18PC mixture. (a): Distribution function for the composition, $\mathscr{P}(x)$ in Eq. (20) (in arbitrary units), and the corresponding free-energy functional, $\mathscr{F}(x)$ in Eq. (21), for a system of linear size $L=10$ at temperature $T=319K$. Results are shown before (- - - -) and after (———) reweighting of the data to a chemical potential corresponding to coexistence. (b) and (c): Size-dependence of the free-energy functional, $\mathscr{F}(x,L)$, and the enthalpy distribution function, $\mathscr{F}(E,L)$, respectively, evaluated at coexistence at temperature $T=319K$. The linear sizes of the systems correspond to $L=5(\square)$, $6(\bigcirc),7(\triangle),8(\triangledown),9(\diamond),10(+)$, and $11(\times)$. For the sake of clarity the different data sets have been shifted vertically.

## B. Phase diagrams

Based on simulation results of the type presented in Figs. 7 and 9 we are able to construct a complete phase diagram for the D14PC-D18PC mixture described by the statistical mechanical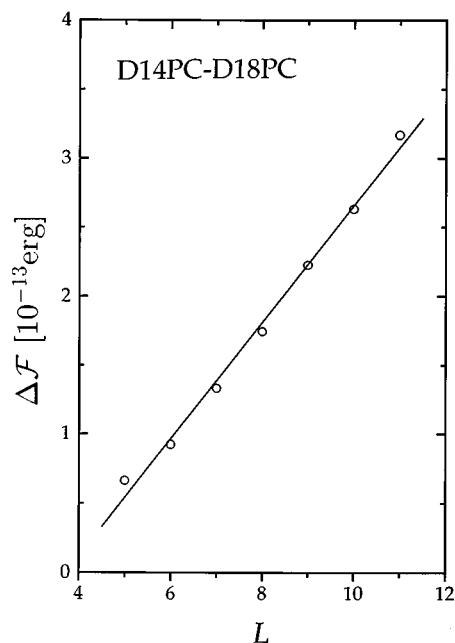 model in Eqs. (1)–(3). This phase diagram, as well as the physical properties associated with the phase lines, has been determined from the data derived from the largest systems that are feasible to treat with current computer resources. These systems are taken to represent the thermodynamic limit. The phase diagram is shown in Fig. 10(a) together with the corresponding diagram derived from mean-field theory using the same value of the mismatch parameter, $\Gamma=0.038\times10^{-13}$ erg/Å, as in the computer simulations. This mean-field phase diagram is different from that presented in Fig. 2(b) because the values used for the mismatch interaction parameter are different. In fact for the higher value of $\Gamma$ the mean-field theory predicts peritectic behavior for the D14PC-D18PC mixture. However, the overall numerical accordance between the accurate Monte Carlo phase diagram and that derived from the approximate mean-field theory is surprisingly good, except for the slope of the solidus (three-phase line). As expected, on the basis of the fact that mean-field theory tends to suppress correlations between fluctuations, there is a close correspondence between mean-field theory and simulation data only in the region of the phase diagram where the mixing of the two lipid components has induced a strong first-order phase transition. Within the mean-field theory there is a first-order phase transition in each of the pure components, whereas the more reliable computer-simulation results predict critical points at low and high contents of D18PC, specifically at compositions $x_{D18PC}\simeq0.08$ and 0.97. The corresponding phase diagram spanned by temperature and chemical potential is shown in Fig. 10(b). In this representation, the critical points are clearly exposed as end points of the line of coexisting phases. Again, a close correpondence between the Monte Carlo and the mean-field results is found for temperatures between the critical points.

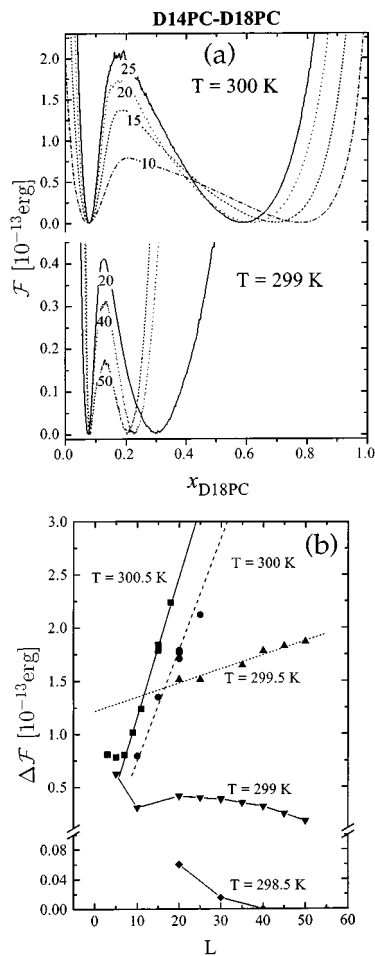The Monte Carlo results for the enthalpy of the coexist-



FIG. 8. Monte Carlo computer-simulation data for the D14PC-D18PC mixture. Dependence of interfacial free energy (the barrier height), $\Delta\mathscr{F}(L)$ in Eq. (22), on the linear size, $L$, of the system. The slope of the solid line is the interfacial tension, $\gamma$, in Eq. (22).

FIG. 9. Monte Carlo computer-simulation data for the D14PC-D18PC mixture. (a): Size dependence of the free-energy functional, $\mathcal{F}(x,L)$. Results are shown for two different temperatures, $T = 299.0$ and $T = 300$ K for a series of different linear lattice sizes, $L$, as indicated on the curves. (b) Size dependence of the free-energy barrier, $\Delta\mathcal{F}(L)$, for temperatures in the vicinity of the critical mixing point.

FIG. 10. Phase diagrams for the D14PC-D18PC mixture. (a): Computer-simulation data for the liquidus ($\square$) and the solidus ($\bigcirc$) lines. The solid lines indicate the corresponding mean-field phase diagram. (b): Computer-simulation results ($\bigcirc$) and mean field results (—) for the phase diagram spanned by temperature, $T$, and chemical potential, $\mu_m$. The positions of critical points corresponding to the Monte Carlo phase diagram are indicated by $*$. Fluid and gel phases are denoted by $\mathbf{f}$ and $\mathbf{g}$. $\mathbf{g}_l$ denotes a gel phase only occurring in the mean-field phase diagram.

ing phases are shown in Figs. 11(a) and 11(b), both as functions of temperature and composition. For comparison, the mean-field results are also given. The discrepancies between the Monte Carlo and mean-field results are largely due to the basic difference in the phase equilibria, in particular with respect to the presence/absence of critical points.

## C. Interfacial tension and compositional fluctuations

The full temperature dependence of the interfacial tension, $\gamma(T)$, is obtained from plots like that displayed in Figs. 8 and 9(b) and is shown in Fig. 12. This figure clearly shows that $\gamma$ vanishes at the critical points, as expected for a second-order phase transition. A maximum of the order $\gamma \simeq 0.6 \times 10^{-13}$ erg/lattice unit ($\sim 10^{-14}$ erg/Å) is attained somewhere in the middle of the temperature range between the two critical points.

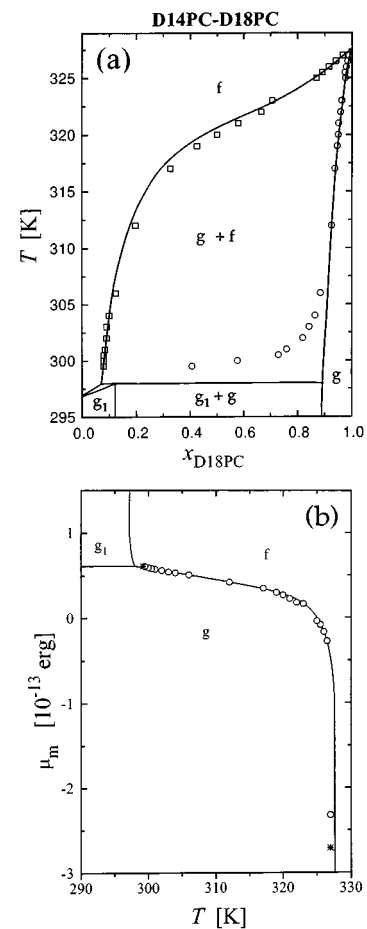In the grand canonical ensemble the composition of a mixture is a fluctuating quantity and a corresponding response function

$$\chi(T) = \left(\frac{\partial^2 G}{\partial\mu^2}\right)_T = (k_B T)^{-1}(\langle x_B^2\rangle - \langle x_B\rangle^2)L^2 \qquad (23)$$

can be defined. $G$ is the Gibbs free energy. It is possible to determine the compositional susceptibility, $\chi(T)$, from the composition distribution function, cf. Fig. 7(a), by separating the histogram into two parts corresponding to the two phases. The value of $\chi(T)$ for an ideal mixture, $\chi_{\text{ideal}}(T)$, along the same $(T,x)$ lines (cf. phase diagram in Fig. 10) can also be calculated. The expression for $\chi_{\text{ideal}}(T)$ is derived by using the relation which connects the second derivatives with respect to the chemical potential and molar fraction of the Gibbs and the Helmholtz free energy, respectively, i.e., $(\partial^2 G/\partial\mu^2)_T = -(\partial^2 F/\partial x^2)_T^{-1}$. The ideal compositional susceptibility can therefore be expressed as $\chi_{\text{ideal}}(T) = (k_B T)^{-1} x_B(1 - x_B)$. Figures 13(a) and 13(b) show the re-
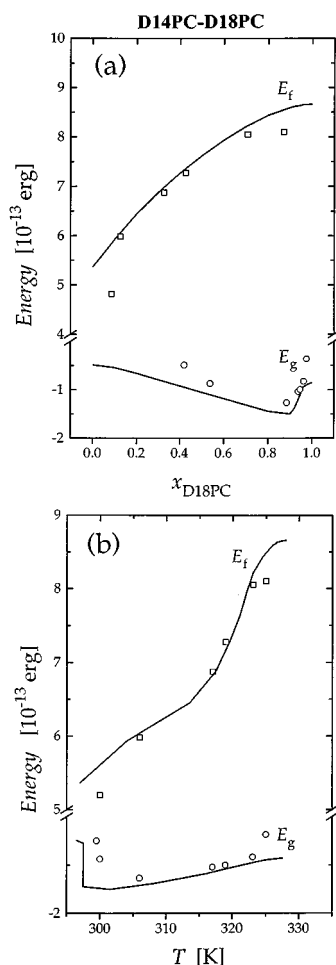
FIG. 12. Monte Carlo computer-simulation data for the interfacial tension, $\gamma$, of the D14PC-D18PC mixture shown as a function of temperature along the coexistence curve. The solid line is a guide to the eye.

FIG. 11. Enthalpy as a function of composition (a) and temperature (b) along the liquidus, $E_f$ ($\square$), and along the solidus, $E_g$ ($\bigcirc$), for a D14PC-D18PC mixture. Monte Carlo data are shown as points and corresponding mean-field data are shown as solid lines.

sults for $\chi(T)$ and $\chi_{ideal}(T)$ along the solidus and liquidus lines, respectively. It is seen from the expression for $\chi_{ideal}(T)$ that the ideal fluctuations reflect the positions of the phase lines in a simple way. $\chi_{ideal}(T)$ is small for small values of $x_A$ or $x_B$ and exhibits a maximum at equimolar composition. For most temperatures, $\chi(T)$ follows the qualitative variation of $\chi_{ideal}(T)$, but $\chi(T)$ is amplified in a nonlinear way compared to $\chi_{ideal}(T)$. This amplification is most pronounced in the gel phase. The similarity between $\chi_{ideal}(T)$ and $\chi(T)$ does not hold near the critical points.

In the fluid phase, strong compositional fluctuations occur near the lower critical point. The fluctuations decrease rapidly and reach a minimum around 300 K corresponding to the steep part of the liquidus line between 10%–20% D18PC, cf. Fig. 10(b). The fluctuations then increase and reach a maximum near 320 K corresponding to the more flat portion of the liquidus line between 40%–60% D18PC, cf. Fig. 10(b). The fluctuations then decrease again. One would then expect that the fluctuations should rise again as the upper critical point is approached. The simulations are not ex-
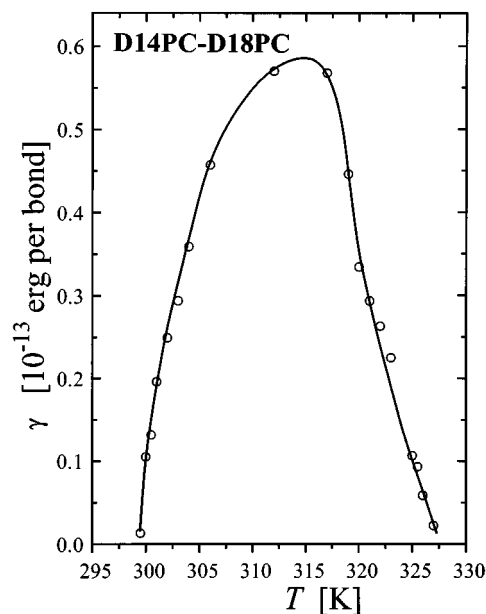
tensive enough to capture this latter feature in the compositional fluctuations. The compositional fluctuations along the solidus, cf. Fig. 13(a), vary very dramatically with temperature and close to the lower critical point they are about two orders of magnitude more intense than those along the liquidus near the critical point. Also the gel-phase compositional fluctuations are expected to blow up near the upper critical point. Similarly to the data for the liquidus, the simulation results along the solidus are not extensive enough to reveal the feature at the upper critical region which appears to be limited to an extremely narrow temperature interval.

## VI. DISCUSSION AND CONCLUSIONS

In the present paper we have presented a mean-field and Monte Carlo simulation study of a statistical mechanical model of the phase equilibria in binary mixtures of saturated phospholipids with mismatch in the hydrophobic acyl-chain lengths. This binary mixture is qualitatively different from that of most other binary mixtures since its properties are strongly influenced by the internal degrees of freedom of the two species. The simulations account accurately for density and compositional fluctuations in the mixture, whereas effects due to fluctuations are to some extent suppressed in the mean-field approximation. However, compared to conventional phenomenological solution theories applied to lipid mixtures, the present mean-field approach captures effects due to the internal degrees of freedom of the acyl chains and it provides independently for a description of the phase behavior of the pure components.

The essential part of the model for the mixture is a term in the Hamiltonian which associates an interaction between
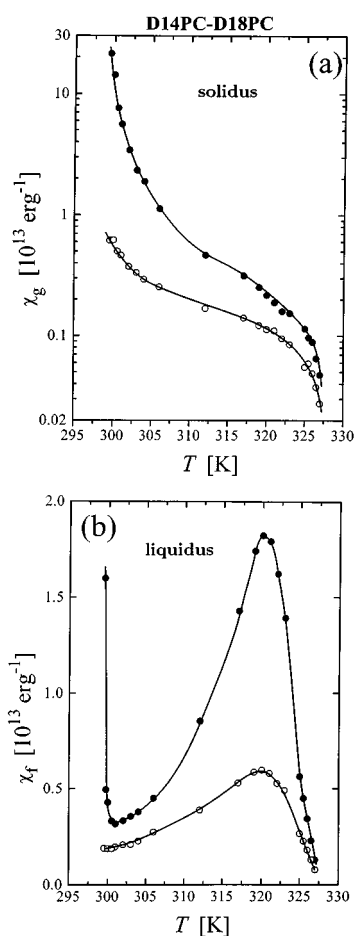
FIG. 13. Monte Carlo computer-simulation data (●) for the compositional fluctuations, $\chi(T)$ in Eq. (23), in the D14PC-D18PC mixture. For comparison is also shown the behavior of $\chi_{ideal}(T)$ corresponding to an ideal mixture (○). Results are given along the coexistence curve for the solidus (a) and the liquidus (b) lines of the Monte Carlo phase diagram [cf. Fig. 10(a)]. The solid lines are guides to the eye.

the two different species which is proportional to the difference in the hydrophobic lengths of the acyl chains. In accordance with an earlier phenomenological model study also built on the concept of hydrophobic mismatch,[38] it is found that the phase equilibria in the homologous series of phospholipid mixtures, D14PC-D16PC, D14PC-D18PC, and D12PC-D18PC, can be described by a single "universal" mismatch parameter, $\Gamma$. The theoretical results show that the phase diagram becomes progressively more non-ideal as the difference in acyl-chain length increases. The overall theoretical predictions of the phase diagrams based on our model calculations are in good agreement with experimental data, considering the uncertainties involved in an experimental determination of lipid phase equilibria using either calorimetric techniques or, e.g., local-probe techniques such as spectroscopies. The nature of the D14PC-D18PC mixture is somewhat controversial and some small-angle neutron scattering results have been interpreted in terms of peritectic behavior.[41]

Our computer simulations of the phase diagrams, which should be considered as very reliable due to the fact that the simulations operate on the free-energy level, reveal some surprising features. They show that whereas within the applied statistical model there is no phase transition in the pure components, such a phase transition and the associated phase equilibria can be induced when two lipid species are mixed. The simulations reveal that the phase diagram for D14PC-D18PC displays a closed coexistence loop with two critical mixing points. It is predicted that these critical points are further removed from the pure-component limits the more closely the acyl-chain lengths are matched. The possibility of occurrence of critical points in these simple two-component phospholipid mixtures has not been previously addressed. There is however no observation in the experimental literature which points to their absence. The published phase diagrams for lecithin mixtures usually do not include data for very dilute mixtures, and the boundaries in the phase diagrams for the less dilute situations have been extrapolated to the pure-component limits under the tacit assumption that the pure components display first-order phase transitions. However, as we have pointed out, no definite experimental proof of the first-order transitional behavior exists. Rather, the most accurate calorimetric work[9] suggests that the transition is at best weakly first order. Our results put the importance of sample impurities into perspective. A small amount of a foreign lipid species (e.g., a lysolipid) in an apparently pure (99%) lipid bilayer may restore the first-order transitional behavior.

The finding that a first-order transition can be induced by mixing lipid species of different chain lengths is probably unique for membrane systems. Usually the opposite is found when other membrane components are mixed in with a lipid bilayer, e.g., cholesterol,[37] polypeptides,[30] or proteins,[33] i.e.. the transition is gradually broadened and removed. Furthermore, our results show that the transition enthalpy in some cases may increase as the pure lipid bilayer is mixed with another component, cf. Fig. 3. When cholesterol, polypeptides, and proteins are incorporated into a lipid bilayer, the transition enthalpy invariably decreases with the concentration. The effect of a long-chain lipid in suppressing the fluctuations in a bilayer composed of lipids with shorter chains is somewhat surprising. One might have expected that the long chain would act as a stiff molecular object at temperatures close to the transition temperature of the short-chain lipid. Hence it appears that the peculiar property of the binary lipid mixture is due to the capacity of lipid acyl chains to adapt to very different environments by undergoing internal conformational changes.

The model calculations of the present paper show that the strong density fluctuations present in pure lipid bilayers become suppressed when the other lipid species is mixed in and at the same time the coexistence is enforced. The weakening of the density fluctuations in the coexistence region is related to the concomitant increase in interfacial tension. The transition enthalpy of the mixture is considerably larger than that predicted for an ideal solution. The contribution to the mixing energy due to the internal conformational degrees of freedom of the acyl chains is quite substantial. To our knowl-

edge there are no systematic experimental measurements of transition enthalpy as a function of composition for the mixtures considered in the present paper. A brief statement in the experimental paper by Mabrey and Sturtevant[6] however indicates that the transition enthalpy obtained from integration of the total excess specific heat for mixtures of D14PC-D18PC is on the average 20% larger than that expected for an ideal mixture. It would clearly be of interest to test experimentally the theoretical predictions of the variation of transition enthalpy shown in Fig. 3.

The model simulations reveal very strong compositional fluctuations in the mixture. These fluctuations are very pronounced near the critical points. Along the liquidus line for D14PC-D18PC the compositional fluctuations display a maximum in the range 40%–60% D18PC which is consistent with a recent study of the local compositional structure in binary lipid mixtures.[34] These strong lateral fluctuations in composition, which persist deep out in the one-phase fluid region, may be of relevance for membrane organization and function.[34]

It is interesting to consider our finding of suppressed density fluctuations in the series of binary lipid mixtures in the context of dynamic lipid-bilayer heterogeneity[14,42,43] which is a term covering the microscopic events accompanying density and compositional fluctuations. Bilayer heterogeneity may be relevant for controlling membrane functions.[43] It is possible that by adding a third lipid component to the mixture, which can mediate the interactions between the two, the density fluctuations may be restored and the phase coexistence be suppressed. The emulsifying effects of such third components are likely to be relevant for biomembrane systems consisting of a large number of different lipid species.

## ACKNOWLEDGMENTS

[1] G. Cevc and D. March, *Phospholipid Bilayers. Physical Principles and Models* (Wiley–Interscience, New York, 1987).

[2] O. G. Mouritsen, Chem. Phys. Lipids **57**, 179 (1991).

[3] M. Bloom, E. Evans, and O. G. Mouritsen, Q. Rev. Biophys. **24**, 293 (1991).

[4] Special Issue on *Phospholipid Phase Transitions*, edited by P. Kinnunen and P. Laggner, Chem. Phys. Lipids **57** (1991).

[5] S. Mabrey and J. M. Sturtevant, Meth. Membrane Biol. **17**, 2464 (1978).

[6] S. Mabrey and J. M. Sturtevant, Proc. Natl. Acad. Sci. USA **73**, 3862 (1976).

[7] M. R. Morrow, R. Srinivasan, and N. Grandal, Chem. Phys. Lipids **58**, 63 (1991).

[8] M. B. Sankaram and T. E. Thompson, Biochemistry **31**, 8258 (1992).

[9] R. L. Biltonen, J. Chem. Thermodyn. **22**, 1 (1990).

[10] D. Chapman, R. M. Williams, and B. D. Ladbrooke, Chem. Phys. Lipids **1**, 445 (1967).

[11] N. Albon and J. M. Sturtevant, Proc. Natl. Acad. Sci. USA **75**, 2258 (1978).

[12] M. R. Morrow, J. P. Whitehead, and D. Lu, Biophys. J. **63**, 18 (1992).

[13] T. Hønger, K. Mortensen, J. H. Ipsen, J. Lemmich, R. Bauer, and O. G. Mouritsen, Phys. Rev. Lett. **72**, 3911 (1994).

[14] O. G. Mouritsen and K. Jørgensen, Chem. Phys. Lipids **73**, 3 (1994).

[15] A. M. Ferrenberg and R. H. Swendsen, Phys. Rev. Lett. **61**, 2635 (1988).

[16] J. Lee and J.M. Kosterlitz, Phys. Rev. Lett. **65**, 137 (1990).

[17] J. Lee and J.M. Kosterlitz, Phys. Rev. B **43**, 3265 (1991).

[18] J. Lee and J. M. Kosterlitz, Phys. Rev. B **43**, 1268 (1991).

[19] J. A. Zollweg and G. V. Chester, Phys. Rev. B **46**, 11186 (1992).

[20] J. Lee and K. J. Strandburg, Phys. Rev. B **46**, 11190 (1992).

[21] R. E. Hetzel, A. Sudbö, and D. A. Huse, Phys. Rev. Lett. **69**, 518 (1992).

[22] S. Chen, A. M. Ferrenberg, and D. P. Landau, Phys. Rev. Lett. **69**, 1213 (1992).

[23] M. Laradji, H. Guo, M. Grant, and M. J. Zuckermann, Phys. Rev. A **44**, 8184 (1991).

[24] Z. Zhang, O. G. Mouritsen, and M. J. Zuckermann, Phys. Rev. Lett. **69**, 2803 (1992).

[25] Z. Zhang, O. G. Mouritsen, and M. J. Zuckermann, Mol. Phys. **80**, 1195 (1993).

[26] Z. Zhang, O. G. Mouritsen, and M. J. Zuckermann, Mod. Phys. Lett. B **7**, 217 (1993).

[27] Z. Zhang, M. Laradji, H. Guo, O. G. Mouritsen, and M. J. Zuckermann, Phys. Rev. A **45**, 7560 (1992).

[28] Z. Zhang, O. G. Mouritsen, and M. J. Zuckermann, Phys. Rev. A **46**, 6707 (1992).

[29] E. Corvera, M. Laradji, and M. J. Zuckermann, Phys. Rev. E **47**, 696 (1993).

[30] Z. Zhang, M. M. Sperotto, M. J. Zuckermann, and O. G. Mouritsen, Biochim. Biophys. Acta **1147**, 154 (1993).

[31] D. A. Pink, T. J. Green, and D. Chapman, Biochemistry **20**, 6692 (1981).

[32] O. G. Mouritsen and M. M. Sperotto, in *Thermodynamics of Membrane Receptors and Channels*, edited by M. Jackson (CRC, Boca Raton, Florida, 1993), p. 127.

[33] O. G. Mouritsen and M. Bloom, Annu. Rev. Biophys. Biomol. Struct. **22**, 147 (1993).

[34] K. Jørgensen, M. M. Sperotto, O. G. Mouritsen, J. H. Ipsen, and M. J. Zuckermann, Biochim. Biophys. Acta **1152**, 135 (1993).

[35] M. M. Sperotto and O. G. Mouritsen, Eur. Biophys. J. **22**, 323 (1993).

[36] O. G. Mouritsen, in *Molecular Description of Biological Membrane Components by Computer Aided Conformational Analysis*, Vol. 1, edited by R. Brasseur (CRC, Boca Raton, Florida, 1990), p. 3.

[37] J. H. Ipsen, O. G. Mouritsen, and M. J. Zuckermann, J. Chem. Phys. **91**, 1855 (1989).

[38] J. H. Ipsen and O. G. Mouritsen, Biochim. Biophys. Acta **944**, 121 (1988).

[39] A. G. Lee, Biochim. Biophys. Acta **472**, 285 (1977).

[40] P. H. von Dreele, Biochemistry **17**, 3939 (1978).

[41] W. Knoll, K. Ibel, and E. Sackmann, Biochemistry **20**, 6379 (1981).

[42] O. G. Mouritsen and K. Jørgensen, BioEssays **14**, 129 (1991).

[43] O. G. Mouritsen and R. L. Biltonen, in *Protein–Lipid Interactions, New Comprehensive Biochemistry*, edited by A. Watts (Elsevier, Amsterdam, 1993), p. 1.